Catalysis Science & Technology

Accepted Manuscript

ROYAL SOCIETY OF CHEMISTRY

www.rsc.org/catalysis

Cite this: DOI: 10.1039/c0xx00000x

www.rsc.org/xxxxxx

ARTICLE TYPE

Vapour phase hydrocyclisation of levulinic acid to γ-valerolactone over supported Ni catalysts

Varkolu Mohan, Velpula Venkateshwarlu, Chodimella Venkata Pramod, Burri David Raju, Kamaraju Seetha Rama Rao*

Received (in XXX, XXX) Xth XXXXXXXXX 20XX, Accepted Xth XXXXXXXXX 20XX
DOI: 10.1039/b000000x

Abstract: Various Ni catalysts with 30 wt% Ni content were prepared by conventional wet impregnation method using different supports such as Al_2O_3, SiO_2, ZnO, ZrO_2, TiO_2 and MgO. The prepared catalysts have been characterised by XRD, N_2 Physisorption, H_2 Pulse chemisorption, Pyridine adsorbed FTIR, Ammonia-TPD, TPR, XPS and TEM techniques. Pyridine adsorbed IR pattern reveals the presence of both Lewis as well as Bronsted acid sites which are responsible for the dehydration of intermediate 4-hydroxy valeric acid to result γ-valerolactone. Ammonia-TPD profiles also showed the presence of acidic sites in all catalytic systems, which explains the formation of targeted product. The better activity showed by 30wt%Ni/SiO_2 catalyst (signifying maximum productivity i.e., 0.8506 kg_{GVL} $kg_{Catalyst}^{-1}$ h^{-1} at 250 °C) is due to the presence of greater number of surface Ni species. The present work is aimed to provide a continuous down flow process for the hydrocyclization of one of biomass derived platform molecule such as levulinic acid over a non-noble metal (nickel) based catalysts. The catalyst is tested for 25h and found to be stable during the time on stream which reveals the robustness of catalyst.

Key words: hydrocyclization, levulinic acid, non-noble metal (nickel), γ-valerolactone.

Introduction:

The non-renewable sources such as fossil fuels are providing around 94% of all our energy needs. The decline of these sources in the near future prompts to search for alternative and renewable sources of fuel. Moreover, the fuels derived from non-renewable sources contribute to global warming by emitting CO_2 to the atmosphere. To overcome this problem one option is to develop alternative strategies with carbon neutral based feed stocks [1, 2]. In this connection, both academia and industry are looking forward to utilise the renewable, carbon neutral biomass to produce bio fuels and value-added chemicals [3, 4]. The advantage of utilization of bio fuel is that the emitted CO_2 can be recycled by the nature via photosynthesis to produce biomass. Among the various biomass derived platform molecules, levulinic acid (LA) is focussed due to its multi-functionalities (keto and acid functional groups) and easy production by the hydrolysis of cellulose and furfuryl alcohol [5 – 7].

The hydrogenation of biomass-derived LA to γ-valerolactone (GVL) is a key reaction in the development of economically realistic and carbon-efficient bio- renewable routes to chemicals and fuel additives [8, 9]. It has recently been suggested that the use of precious metal catalysts is detrimental to the overall process economics for the production of GVL in the industry [10-13]. In spite of having good catalytic performance, cost factor of these catalysts, usage of volatile organic additives, high pressure operations and involvement of other harsh reaction parameters limits their application in the industry. Although some of the Ni catalysts such as Raney Ni and Urushibara Ni catalysts are reported for the hydrogenation of LA to yield GVL, these catalysts exhibited low yields [14]. Upare et al. studied the same reaction at 265 °C and 25 bar pressure over silica supported copper catalysts and observed that the decline in activity during the time on stream. To overcome the deactivation during time on stream, the catalyst has been promoted with Ni [15]. In a patented work over Ni catalyst, 71 % yield of GVL has been achieved by Haan et al [16]. Thus, hydrocyclisation of LA by non-noble metal (Ni) catalysts gained importance in recent times.

So far, no report has been reported for the LA hydrocyclisation over Ni catalysts in vapour phase at atmospheric pressure. This investigation highlights the effect of supports on catalytic performance of LA hydrocyclisation over supported Ni catalysts at atmospheric pressure without using any organic additives.

Experimental:

Preparation of various supported Ni Catalysts:

Commercial supports such as Al_2O_3 (M/s. SudChemie, India), SiO_2 (M/s. Aldrich Chemicals, USA), MgO, TiO_2, ZnO and ZrO_2 (M/s.Sd fine India Ltd, India) were used without further purification. Briefly, the method of preparation involves soaking the support in aqueous $Ni(NO_3)_2 \cdot 6H_2O$ (M/s. Sd fine India Ltd) solution followed by drying at 80 °C. The resultant solid was dried at 100 °C for 12 h and, then calcined in air at 450 °C for 5 h. The amount of Ni loading was fixed at 30 wt %. The prepared catalysts are designated as NA, NM, NS, NT, NZn and NZr for Ni/ Al_2O_3, Ni/MgO, Ni/ SiO_2, Ni/ TiO_2, Ni/ZnO and Ni/ZrO_2 respectively.

Characterization:

X-ray diffraction patterns were recorded on a Ultima-IV (M/s. Rigaku corporation, Japan) XRD unit operated at 40 kV and 40 mA equipped with nickel-filtered Cu Kα radiation (λ = 1.54056 Å) and a 2θ value ranging from 2 to 80° at a scanning rate of 0.02°/step. N_2 physisorption studies were determined using a Quadrasorb analyzer (M/s. Quanta Chrome instruments, USA) by nitrogen adsorption at −196 °C. The specific surface areas were calculated by using the BET method. FTIR spectra of pyridine adsorbed catalysts were recorded by ex-situ method on a Spectrum

GX spectrometer (M/s. Perkin–Elmer, Germany) at room temperature. 10 mg of the each catalyst was oven dried at 100 °C for 1 h. To this oven dried catalysts, 0.1 ml of pyridine was added, followed by vacuum drying at 120 °C for 1h to remove the physisorbed pyridine[17]. The samples were finely ground and dispersed in KBr (1:10 ratio). The spectral resolution was 4 cm^{-1} in the spectral range 400-4000 cm^{-1}, and 10 scans were recorded for each spectrum.

H_2 – Chemisorption measurements using pulse (100µL) titration procedure was carried out at 40 °C on a AUTOSORB-iQ, automated gas sorption analyser (M/s. Quantachrome Instruments, USA) in order to obtain the dispersion and metal particle size, metal surface area of the catalyst. Prior to the experiment, the catalyst was reduced at 500 °C for 2 hrs followed by evacuation for another 2 hrs to remove any physisorbed hydrogen present on the catalyst surface. The monolayer uptake (Nm), Active Metal surface Area (AMSA), Metal dispersion (D) and particle size (d) was calculated by TPRWin software.

Temperature programmed reduction (TPR) of the catalysts was carried out in a flow of 5% H_2/Ar mixture gas at a rate of 30 cm^3min^{-1} with a temperature ramping of 10 K min^{-1}. The hydrogen consumption was monitored using a thermal conductivity detector (TCD) and a GC software Class-5000 on a 17A gas chromatograph (M/s. Shimadzu Instruments, Japan). The XPS analysis was performed using a AXIS 165 apparatus (M/s.Kratos Instruments, UK) equipped with a dual anode (Mg and Al) using Mg Kα source. The non monochromatized Al Kα X-ray source ($h\upsilon$ = 1486.6 eV) was operated at 12.5 kV and 16 mA. Analysis was done at room temperature and prior to analysis the samples were maintained under rigorous vacuum typically in the order of 10^{-8} Pa to avoid the amount of contaminates.

The acidity of the catalysts were measured by temperature programmed desorption of NH_3 using AUTOSORB-iQ, automated gas sorption analyser (M/s. Quantachrome Instruments, USA). Prior to desorption, the catalyst has been saturated with the NH_3 at 80 °C for 0.5 h, followed by stripping with Helium for 0.5 h to remove the physisorbed NH_3 at the same temperature. Then, the temperature was raised to 800 °C at 10 ºC min^{-1} and the desorbed NH_3 was monitored of with the inbuilt TCD in a flow of Helium (60 ml min^{-1}).

Activity Test:

Catalytic tests were conducted at the atmospheric pressure in a fixed-bed reactor (14mm id and 300 mm length) made up of quartz glass with 1g catalyst particles mixed with same amount of quartz particles placed at the centre of the reactor. In order to get vaporization of reactant before contacting the catalyst, a layer of silicon beads served as a preheating zone (50mm long) have been placed above the catalyst bed and a temperature of 250 °C was maintained.Prior to the test, the catalyst was reduced at 500 °C for 4 h in a flow of H_2 (1800 ml h^{-1}). The liquid feed (LA) was fed continuously at a rate of 1ml h^{-1} using a syringe feed pump (M/s. B.Braun Co., Germany). H_2 feed was also maintained along with LA feed by keeping the H_2/ LA molar ratio as 8. The products were collected in an ice cooled trap and analyzed by flame ionization detector (FID) equipped gas chromatograph, GC-17A (M/s. Shimadzu Instruments, Japan). The product components were confirmed by QP5050 GC-MS (M/s. Shimadzu Instruments, Japan).

The conversion, selectivity and yield were calculated as follows:

$$\text{Levulinic acid conversion (\%)} = \frac{\text{levulinic acid in feed} - \text{levulinic acid in the sample}}{\text{levulinic acid in feed}} X100$$

$$\text{GVL Selectivity (\%)} = \frac{\text{GVL produced}}{\text{levulinic acid converted}} X100$$

$$\text{GVL Yield(\%)} = \text{Levulinic acid conversion X GVL Selectivity X100}$$

Results and discussion:

In order to elucidate the influence of support, various supported Ni catalysts viz., NA, NM, NS, NT, NZn and NZr are tested for the hydrocyclization of biomass derived levulinic acid to γ-valerolactone with H_2/LA molar ratio of 8 in the vapour phase at 250°C at atmospheric pressure and the data is displayed in Figure-1. The data in Figure-1 clearly indicates that the NS is an efficient catalyst for the hydrocyclization of the levulinic acid. The lower conversions of LA over NZr, NZn and NT catalysts are not surprising, because these catalytic systems showed lower Ni dispersions (Table-1). The lower catalytic activity of NZr, NZn and NT catalyst systems is thus due to the presence of fewer number of surface Ni species.

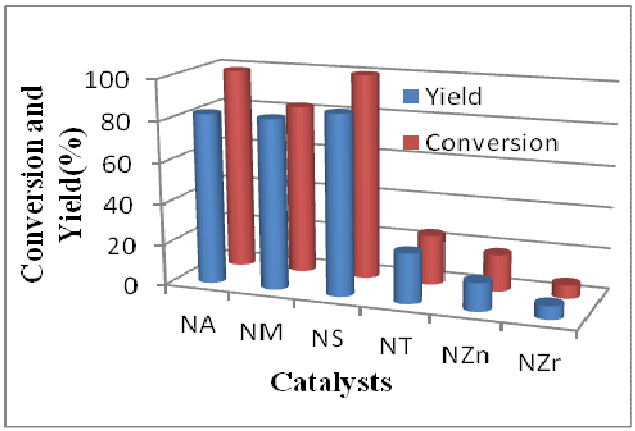

Figure-1. Variation of the conversion and yield against all the Ni based catalysts. Reaction Conditions: Weight of the catalyst=1 g, Temperature=250 °C, Pressure=1 atm, Levulinic acid = 1 ml h^{-1}, carrier gas (H_2) = 1800 ml h^{-1}, H_2/LA molar ratio = 8.

BET surface area values of the catalysts are summarized in Table-1. The BET surface area of NS and NA are more or less the same (135 and 134 m^2g^{-1}). BET area of NZr is 87 m^2g^{-1}. BET surface area of NM, NT and NZn are low. H_2 chemisorption results are summarized in Table-1. The active Ni metal surface area (AMSA) decreases in the following order: NS > NA > NM > NZn > NZr ≈ NT. Lower AMSA values and bigger Ni particles (d) observed on NT, NZn and NZr which can be ascribed to considerable nucleation and rapid aggregation leading to the formation of large Ni crystallites. The Ni dispersion (D) is in line with AMSA values. These observations suggest that the low surface area of the support favors poor Ni dispersion (Table-1). Although, MgO possesses low surface area, the Ni dispersion is higher than that in the catalysts NT, NZn and NZr which may be due to similar structural integrity (Both are having fcc structure).

Catalyst	SA (m^2/g)[a]	Acidity (µmoles/ g)[b]	Nm (µmoles/ g)[c]	AMSA (m^2/g_{Ni})[c]	d (nm)[c]	D (%)[c]
NA	134	190	165.9	13.0	15.6	6.5
NM	15	20	101.9	8.0	25.4	4.0
NS	135	62	195.0	15.3	13.3	7.6
NT	7	30	40.0	3.1	64.6	1.6
NZn	6	99	83.5	6.5	30.9	3.3
NZr	87	113	39.5	3.1	65.5	1.5

Table-1.Physico-chemical properties of all the nickel based catalysts. [a] BET surface area determined from N_2 gas adsorption,[b] Calculated from NH_3-TPD, [c] Calculated by H_2-pulse chemiorption

XRD patterns of all the calcined catalysts are shown in Figure-2. The presence of NiO phase in the calcined catalysts suggests the decomposition of nickel nitrate in air during the calcination to form the NiO species. The XRD profile of the Ni/SiO_2 catalyst presents a broad peak at a 2θ value of 22° which is assigned to amorphous silica [18]. According to the literature, the reflections at 2θ = 36.65 (111), 42.70 (200), 62.25 (220), 74.83(311) and 79.23 (222) ° (ICDD No. 88-2326) can be ascribed to the NiO phase in all the catalysts. The reflections at 2θ = 37.28 and 62.8° can be attributed to nickel silicate in NS catalyst[19]. Valentini et al reported that the diffraction pattern of the Ni/Al_2O_3 catalyst is not easy to clearly discriminate NiO, $NiAl_2O_4$ and γ- Al_2O_3 due to their close proximity of their crystal structure. However, the TPR pattern (Figure-6) of Ni/Al_2O_3 clearly justifies the formation of $NiAl_2O_4$ [20]. The diffraction pattern of the Ni/ZnO catalyst shows the wurtzite structure of ZnO at 2θ reflections of 37.2 and 43.28° [21]. The XRD profile of the Ni/MgO catalyst shows peaks at 2θ =37, 43, 62.4 and 66° which can be ascribed to either MgO or $MgNiO_2$ phases [22, 23] which possess same crystal structure (both MgO and Ni having face centred cubic structure) . Peaks at 2θ = 30.3, 35.14, 50.48 and 60.2° reveal the presence of indices (111), (200), (220) and (311) planes, respectively (cubic ZrO_2, Space group Fm3m (225) with a lattice parameter of 0.509 nm) (ICDD.No.27-0997) [24]. The peaks at 2θ = 25.32, 37.84, 48.07, 53.95, 55.10, 62.16, 70.34 and 75.12° reveal the presence of indices (101), (004), (200), (105), (211) (Tetragonal TiO_2, Space group 14_1 / amd (141)) corresponding to titania (anatase) (ICDD .No.84-1286).

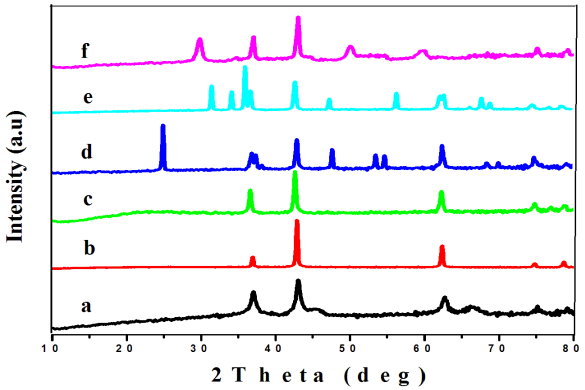

Figure-2: XRD profiles of Calcined catalysts (a) NA (b) NM (c) NS (d) NT (e) NZn (f) NZr.

XRD patterns of all the reduced catalysts are shown in Figure-3. All the reduced catalysts showed the XRD reflections indexed at 44.49° (111), 51.85° (200) and 76.38° (220) corresponding to metallic Ni with face centred cubic geometry of the space group Fm3m (225) with cell parameter 3.523 A° (ICDD.No.87-0712) except NM and NZn patterns wherein slight distortions were observed. These reflections in case of NM at 2θ values of 37.04, 62.49, 78.88 may be due to the presence of $NiMgO_2$ (ICDD No.24-0712) or MgO. It is well known that the XRD patterns of the (Mg, Ni)O system ($MgNiO_2$) phase (cubic system, spatial group Fm3m and parameter a = 4.1922 A^0), its structural integrity is similar to that of MgO (cubic system, spatial group Fm3m, parameter a = 4.209 A °) phase [23]. From the pulse chemisorption it is clear that the Ni particles in NM are in dispersed form than that in NZn, NZr and NT catalysts.

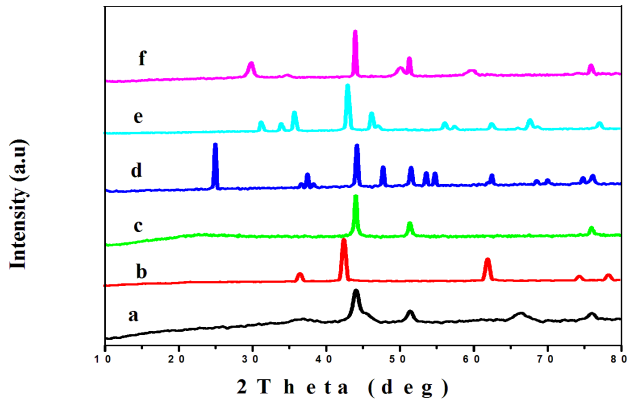

Figure-3: XRD profiles of reduced catalysts (a) NA (b) NM (c) NS (d) NT (e) NZn (f) NZr.

Pyridine adsorbed IR patterns of Ni catalysts are shown in Figure-4. From these patterns, one can find out the acidity of the catalysts. In all the patterns, the bands at 1445 cm^{-1} and 1490 cm^{-1} are ascribed to the Lewis acid sites and combination of Bronsted & Lewis acid sites respectively [25, 26].

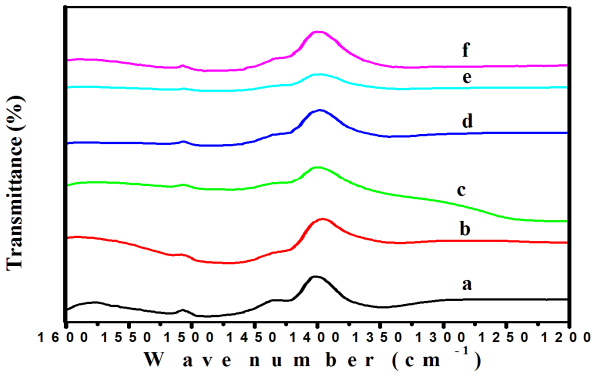

Figure-4. Pyridine adsorbed IR patterns of all the Ni based catalysts (a) NA (b) NM (c) NS (d) NT (e) NZn (f) NZr.

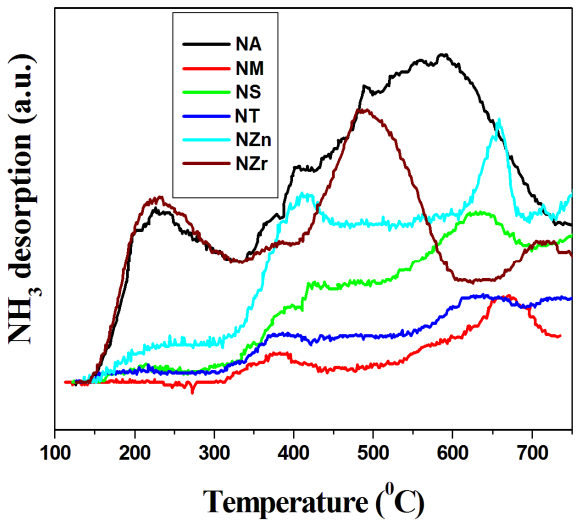

Figure-5. NH_3-TPD patterns of supported Ni catalysts.

The temperature programmed desorption of ammonia (NH_3- TPD) profiles of the catalysts are shown in Figure-5, and the acidity values are summarised in Table-1. The acid site distributions mainly classified by temperature range like weak (< 250 °C), medium (250-400 °C) and strong (> 400 °C) acidic sites[27]. The NA catalyst showed three desorption peaks around at 200°C , 480 °C and 550° C indicating that the presence of weak and strong acidic sites with a total acidity of 190 µmoles/g. The NZn catalyst also showed two desorption peak centred at 400 °C and 650 °C signifying the existence of both medium and strong acidic sites with a total acidity of 99 µmoles/g. The NS, NT, NM catalysts also illustrated two desorption peaks centred at 380 and 650 °C endorsed to the presence of medium and strong acidic sites with a total acidity of 62, 30 and 20 µmoles/g respectively. The NZr catalyst also recognized by two desorption peaks centred at 380 and 650 °C respectively with an acidity of 113 µmoles/g. The acidity of catalytic systems play a key role to the dehydration of intermediate (4-hyroxy valeric acid). However, formation of 4-hyroxy valeric acid requires good number of Ni sites with smaller particle size. Eventhough, NZn, NT and NZr possess greater number of acidic sites than that in NM, these catalysts fail to yield good conversion because of the presence of bigger Ni particles. It is fact that the supported Ni catalyst with lower Ni content possesses higher Ni dispersion. However, as the Ni content increases number of surface Ni sites increases upto certain loading .This was demonstrated in our earlier publication in which 30 wt% Ni was found to be optimum in Ni/HZM-5 catalysts[28].

TPR results yield an insight for the supported metal catalysts regarding the metal-support interactions and also the temperatures at which the metal oxide gets reduced to metal. The TPR profiles of the nickel-based catalysts are shown in Figure- 6. Fajardo *et al.* observed that the peak centred at around 820°C in the TPR pattern of NA catalyst is due to the reduction of $NiAl_2O_4$ spinel structure which clearly demonstrates the presence of a strong metal-support interaction [29]. In the present situation also, the presence of a shoulder peak at >800 °C due to the presence of NiO-Al_2O_3 interacted species and another peak at >500 ° attributed to the reduction of weak interacted species with the Al_2O_3 are observed. In case of NM catalyst, a broad peak was observed that could be attributed to the reduction of $MgNiO_2$ formed due to strong interaction of MgO with Ni spieces [23, 30]. In the literature, it is reported that in the TPR pattern of Ni/MgO catalyst showed three reduction peaks at a T_{max} of 325, 600 and 775°C due to the reduction of NiO located on the MgO surface, some form of Ni^{2+} ions having square-pyramidal coordination in the outermost layer of the catalyst structure, and the NiO–MgO ($MgNiO_2$) solid solution lattice respectively [31]. The defect sites of MgO may be responsible for the presence of strongly adsorbed Ni species on MgO [32]. Pompeo *et al*. suggested that the TPR pattern of the Ni/SiO_2 catalyst shows two reduction peaks at T_{max} of around 450 and 610°C . The low temperature signal is due to the weakly interacted NiO species with the support and a similar observation is found in the present study. The presence of the signal at T_{max} of 610°C is due to nickel oxide interacting chemically with the support and is not observed in the present investigation [33]. In the TPR pattern of NT, only one broad reduction peak observed in the range of 380 to 500° C is due to the reduction of bulk NiO [34]. Yang *et al*. reported the presence of two reduction peaks at around 480 and 620°C in the TPR pattern of Ni/ZnO catalyst. The low temperature signal can be assigned to the reduction of bulk NiO species which are in weak interaction with ZnO surface, while the peak at around 620°C can be attributed to the reduction of Ni ions that are interacted strongly with the zinc oxide support [35]. A Similar TPR findings are observed in the present study with NZn catalyst. In the case of NZr, reduction peaks with T_{max} at about 443° C is observed and it can be assigned to relatively free NiO species [36].

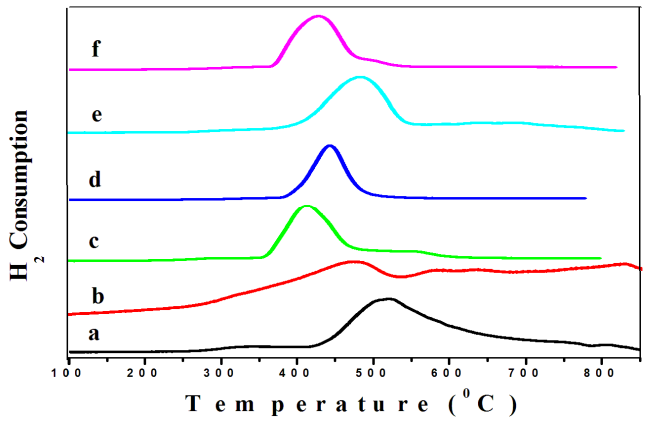

Figure-6: TPR profiles of all the Ni based catalysts (a) NA (b) NM (c) NS (d) NT (e) NZn (f) NZr.

The XPS spectra of NS catalysts (reduced and spent) are shown in Figure-7. The reduced catalyst shows two major peaks at binding energies (BE) of 852.8 and 869.7 eV corresponding to the core level Ni $2P_{3/2}$ and Ni $2P_{1/2}$ transitions respectively. Some part of the Ni in the catalyst might have undergone surface oxidation resulting in yielding two shoulder peaks at binding energies (BE) of 858 and 874 eV in the XPS pattern [37]. The difference between two peaks of Ni^0 metal (≈17.2 eV) is very close to the reported value [38]. Similar XPS pattern was observed in case of spent catalyst. This clearly indicates that there is no change in the oxidation state of Ni during the reaction. The TEM image (Figure -8) clearly indicates that the metal particles are in highly dispersed form.

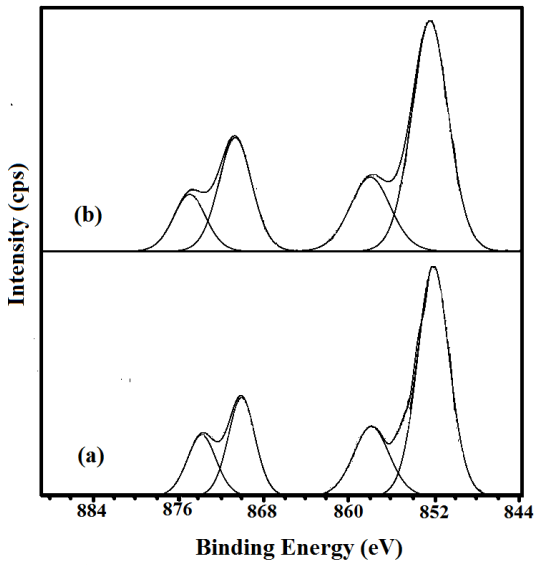

Figure-7. XPS pattern of NS catalyst (a) reduced (b) spent

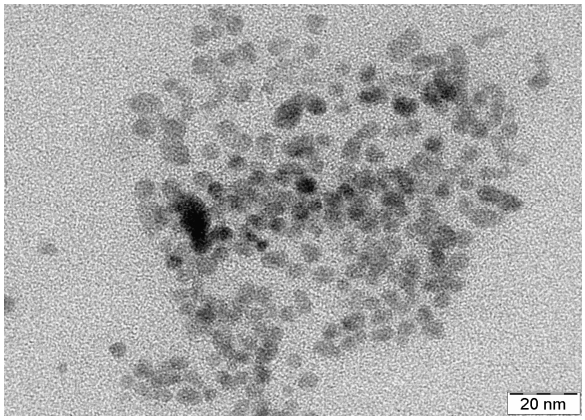

Figure-8. TEM image of NS catalyst.

To study the reaction mechanism (Scheme-1), the reaction product components have been monitored by GC-MS. However, the intermediate, 4-hydroxy valeric acid could not be traced because of its highly unstable nature and due to which it easily lose water molecule to produce GVL [39, 40]. Presence of strong acidic sites in the catalyst favours path I. This observation was evidenced in our recently published Ni/HZSM-5 catalyst [28]. The absence of angelica lactone, the intermediate in reaction path I over the catalysts of present investigation clearly indicates that the reaction proceeds via path II. The Pyridine adsorbed IR patterns also suggests that the Lewis and combination of Lewis and Bronsted acid sites which are responsible for the dehydration of intermediate (4-hydroxy valeric acid). To elucidate the mechanism, the reaction was carried out over bear supports and observed a maximum of 5 % conversion of Levulinic acid over Al_2O_3 and on other supports, no appreciable conversion of levulinic acid was observed. Angelica lactone is the only product observed over Al_2O_3. From the pyridine adsorbed FTIR and TPD of NH_3, it can seen that the all the catalytic systems have the acidity which is playing crucial role in the dehydration of intermediate (4-hydroxy valeric acid). However the number of these acidic sites is not enough to yield angelica lactone which clearly ruled out path-I in Scheme-1.

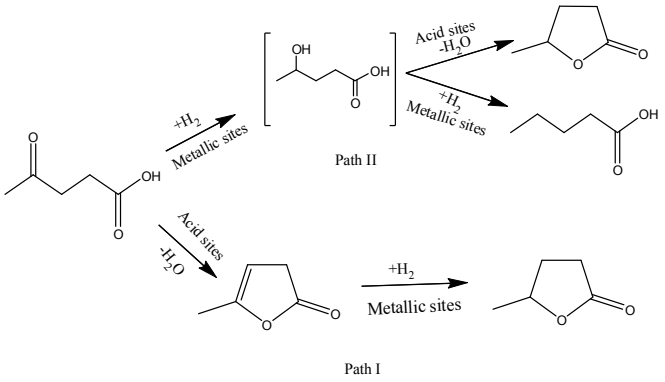

Scheme-1.Plausible reaction scheme for the levulinic acid hydrogenation over Ni based catalysts.

It is well known that in the hydrogenation reaction, first step is chemisorption of molecular hydrogen and LA (Scheme-2) [14, 41, 42]. Dissociative chemisorption of H_2 over Ni catalysts is known and this is helpful in transfer of that adsorbed atomic hydrogen to keto group of LA which is present on the same surface/adjacent surface site, resulting in the formation of intermediate (4-hydroxy valeric acid) [14, 43]. Further hydrogenation of these intermediate results in the formation of valeric acid in small amounts and the presence of acidic sites in the catalyst promotes GVL formation through self condensation [43, 44].

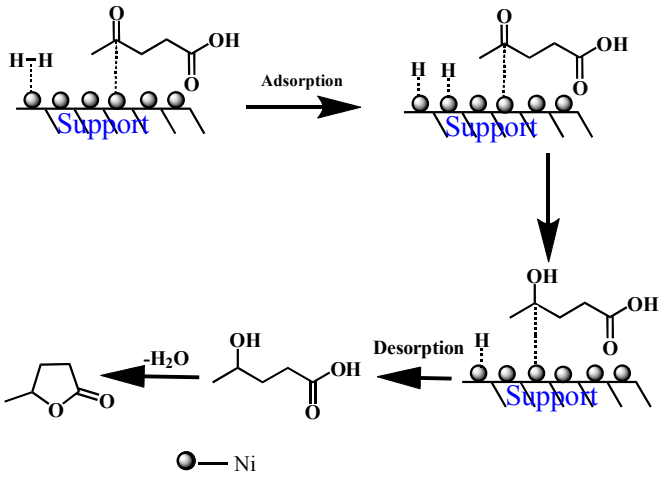

Scheme-2. Hydrogenation pathway of LA to GVL on NS catalyst.

As Levulinic acid is a biomass derived product, the influence of impurities in the feed was performed over NS catalyst. The reaction with co –feeding of formic acid and levulinic acid (1:1 molar ratio) in N_2 flow (30 ml) yielded 37% conversion of levulinic acid with a 22 % yield of gamma valerolactone. Furthermore, we also performed the reaction with co-feeding of water (1:1 molar ratio) in H_2 flow with similar reaction conditions. No significant change in activity with the co-feeding of water (87% yield of gamma valerolactone) was observed. A similar observation was reported earlier with nitrobenzene-water mixture over a Ni/SBA-15 catalyst yielding ~90 % yield of aniline which indicated the robustness of the silica material [23].

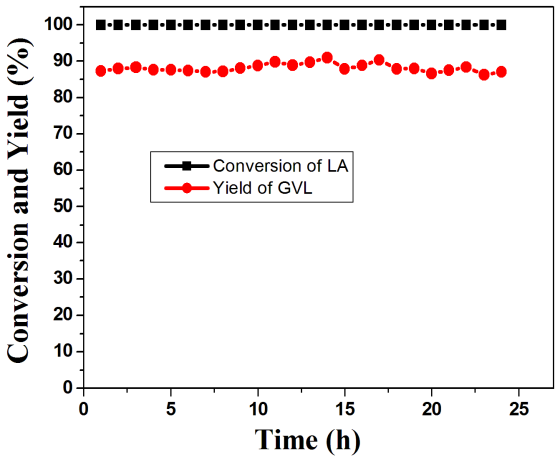

Figure-9. Influence of time on stream over NS catalyst at 250°C, WHSV=1.

The time on stream analysis was carried out for a period of 25h over NS catalyst with optimised reaction conditions (Temperature 250 °C, 1 atmosphere) to evaluate the steadiness of the catalyst. The result was presented in Figure-9. The consistent activity was observed during the whole period. The yield towards the GVL is also constant during the entire course of the reaction. In our earlier work, we observed the decline in conversion as well as yield due to fouling of reaction intermediate [28]. Both the fresh and spent catalysts were analysed by Atomic Absorption Spectroscopy (AAS) to observe the composition of Ni and found that there no leaching of Ni. The reliable catalytic activity of NS can be owing to the large number surface Ni species and also Lewis acidity. This explains the robustness of catalytic system.

Productivity of NS catalyst is calculated and compared with other catalysts reported in recent literature on this reaction [15, 45]. The conditions for the catalytic activity of reported catalysts were 265 °C at atmospheric pressure. The productivity of our catalytic system, NS is higher (0.8506 $Kg_{GVL}Kg_{catalyst}$ h^{-1}) and follows the order: Ni/HZSM-5 (0.9090) [28] > **NS (0.8506)** > NA (0.81055) > NM (0.80079) > 5%Ru/C (0.4545) [45] > 5%Cu/SiO_2 (0.4444) [15] > 5%Pd/C (0.4040) [45] > 5%Pt/C (0.1515) [45].

Conclusion:

In summary, 30 wt% Ni/SiO_2 is found to be an efficient and environmentally benign catalyst for the hydrocyclization of levulinic acid to GVL. Among all the catalytic systems, NS shows good productivity (0.8506 $Kg_{GVL}Kg_{catalyst}$ h^{-1}) at 250°C, 1 atmospheric pressure due to large number of surface Ni species. Furthermore, the catalyst is stable upto 25h during time on stream without any deactivation in catalytic activity. The catalyst possesses higher productivity in comparison with the reported catalysts. This clearly indicates the sturdiness of NS catalyst.

Acknowledgements

Authors, VM, CVP and VV thank CSIR and UGC, New Delhi respectively for the award of fellowship.

Notes and references

Inorganic and Physical Chemistry Division, CSIR-Indian Institute of Chemical Technology, Hyderabad, India-5000071, E-mail: ksramarao@iict.res.in Fax: +91-40-27160921; Tel: +91-40-27191712

1. D. L. Klass, Biomass for Renewable Energy, Fuels, and Chemicals, Elsevier, Amsterdam, 1998.
2. J. Chow, R. J. Kopp and P. R. Portney, *Science*, 2003, **302**, 1528.
3. A. J. Ragauskas, C. K. Williams, B. H. Davison, G. Britovsek, J. Cairney, C. A. W. J. Frederick Jr., J. P. Hallett, D. J. Leak, C. L. Liotta, J. R. Mielenz, R. Murphy, R. Templer, T. Tschaplinski, *Science*, 2006,**311**,484.
4. G. W. Huber and A. Corma, *Angew. Chem., Int. Ed.*, 2007,**46**, 7184.
5. D.J. Hayes, S. Fitzpatrick, M.H.B. Hayes, J.R.H. Ross, in: B. Kamm, P.R. Gruber, M.Kamm (Eds.), Biorefineries—Industrial Processes and Products, vol. 1, Wiley- VCH, Weinheim, 2006, p. 139.
6. D.J. Hayes, *Catal. Today*, 2009,**145**,138.
7. Z.S.He.,*Chemical Industry and Engineering*, 1999,**2**,163.
8. I. T. Horvath, H. Mehdi, V. Fabos, L. Boda and L. T. Mika, *Green Chem*., 2008,10,238.
9. L. E. Manzer, *Applied Catalysis A: General*, 2004,**272**,249;
10. L. Bui, H. Luo, W. R. Gunther, and Y. Roman-Leshkov, Angew. Chem. Int. Ed. 2013, **52**, 8022.
11. D. J. Braden, C. A. Henao, J. Heltzel, C. C. Maravelias, J. A. Dumesic, Green Chem. 2011, **13**, 1755.
12. S. M. Sen, D. M. Alonso, S. G. Wettstein, E. I. G_rb_z, C. A. Henao, J. A. Dumesic, C. T. Maravelias, Energy Environ. Sci. 2012, **5**, 9690;
13. K. Yan, J. Liao, X. Wu, X. Xie, RSC Adv. 2013, **3**, 3853.
14. Z.Yan, L. Lin, S. Liu., *Energy & Fuels,* 2009,**23**,3853.
15. P. P. Upare, Jong-Min Lee , Y. K.Hwang, D. W. Hwang ,Jeong-Ho Lee, S. B. Halligudi ,Jin-Soo Hwang , Jong-San Chang.,*ChemSusChem*, 2011,**4**,1749.
16. R. J. Haan, J. P. Lange, L. Petrus, C. J. Maria, P.H. Legal, US Patent No. 0208183A1, 2007.
17. C. R. Reddy, Y. S. Bhat, G. Nagendrappa and B. S. Jai Prakash, Catal. Today, 2009, **141**, 157.
18. R. M.Rioux, H.Song, J. D. Hoefelmeyer, G. A.Somorjai, *J. Phys.Chem.B* , 2005,**109,**2192.
19. R. Takahashi, S. Sato, T. Sodesawa, S. Tomiyama, *Appl.Catal. A: Gen.,* 2005, **286**,142.
20. A. Valentini, N.L.V.Carreno, L.F.D. Probst, P.N. Lisboa-Filho, W.H. Schreiner, E.R. Leite, E. Longo , *Appl.Catal. A: Gen*, 2003,**255**,211.
21. C.J.Cong, J.H. Hong, Q.Y. Liu, L. Liao, K.L.Zhang, Solid State Commun , 2006,**138**,511.
22. T. Furusawa, A. Tsutsumi ,Appl. Catal. A ., 2005,**278**, 207.
23. V. Mohan, C. V. Pramod, M. Suresh, K. Hari Prasad Reddy, B. David Raju, K. S. Rama Rao, *Catal. Commun*, 2012, **18**, 89.
24. S. K. Das, M. K. Bhunia, A. K. Sinha and A. Bhaumik, *J. Phys. Chem. C*, 2009,**113**, 8918.
25. J.C. Vedrine, A. Aurox, V. Bolis, *J. Catal*. 59(1979) 248-262.
26. N.Y. Topsoe, K. Pdersen, E. Derouane, *J. Catal*, 1981,**70**,41.
27. A. Boreave, A. Auroux, C. Guimon, Microporous Mater. 1997, **11**, 275.
28. M. Varkolu, R. Chakali, V. P. Chodimella, D. R. Burri , R. R. S. Kamaraju, *RSC Adv.*, 2013, DOI: 10.1039/C3RA46485G.
29. H.V. Fajardo, A.O. Martins, R.M. Almeida, L.K.Noda, L.F.D.Probst, N.L.V.Carreno, A. Valentini,*Mater. Lett*, 2005, **59**, 3963.
30. S. Tang, J. Lin, K.L. Tan, *Catal.Lett.*, 1998, **51**, 169.
31. T. Furusawa, A. Tsutsumi, *Appl. Catal. A*, 2005, **278**, 207.
32. A.V. Matveev, K.M. Neyman, I.V. Yudano, N. Rosch, *Surface Science*, 1999,**426**,123.

33. F.Pompeo, N.N.Nichio, M.G.Gonzalez, M.Montes, *Catal. Today* , 2005,**107–108**,856.
34. S.W.Ho, C.Y.Chu, S.G.Chen, *J. Catal.*, 1998,**178**,34.
35. Y.Yang, J. Ma, F.Wu, *Int J Hydrogen Energy*, 2006,**31**, 877.
36. Hyun-Seog Roh, K.Y.Koo,J. H. Jeong,Y. T.Seo,D. J. Seo,Yong-Seog Seo,W. L. Yoon, , S. B. Park , *Catal. Lett.*, 2007,**117**, 85.
37. D. Datta,B.J.Borah,L. Saikia,M.G.Pathak,P. Sengupta, D.K. Datta, *Applied Clay Science,* 2011,**53**, 650.
38. S. Xiao, Z. Meng, *J. Chem. Soc. Faraday Trans*, 1994, **90**, 2591.
39. R. T. Morrison , R. N. Boyd, Organic Chemistry, Allyn and Bacon, Boston, 1983, **20,** 813.
40. D. M. Alonso, S. G. Wettstein, J. A. Dumesic, *Green Chem*., 2013, **15**, 584.
41. W.R.H.Wright, R. Palkovits, ChemSusChem, 2012, **5**, 1657.
42. D.M. Alonso, S.G. Wettstein, J.Q. Bond, T.W. Root, J.A. Dumesic, ChemSusChem, 2011,**4**,1078.
43. J.C. Serrano-Ruiz, D.J. Braden, R.M. West, J.A. Dumesic, Appl. Catal. B ,2010,**100**, 184.
44. F.M.A. Geilen, B. Engendahl, M. Hölscher, J. Klankermayer, W. Leitner, J. Am.Chem. Soc, 2011,**133**, 14349.
45. P. P. Upare, Jong-Min Lee , D. W. Hwang , S. B. Halligudi , Y. K.Hwang, Jong-San Chang., *J. Ind. Eng. Chem.,* 2011,**17**, 287.

Vapour phase hydrocyclisation of levulinic acid to γ-valerolactone over supported Ni catalysts at atmospheric pressure

Varkolu Mohan, Velpula Venkateshwarlu, Chodimella Venkata Pramod, Burri David Raju, Kamaraju Seetha Rama Rao*

Inorganic and Physical Chemistry Division, CSIR-Indian Institute of Chemical Technology, Hyderabad, India-5000071, E-mail: ksramarao@iict.res.in Fax: +91-40-27160921; Tel: +91-40-27191712

Graphical abstract:

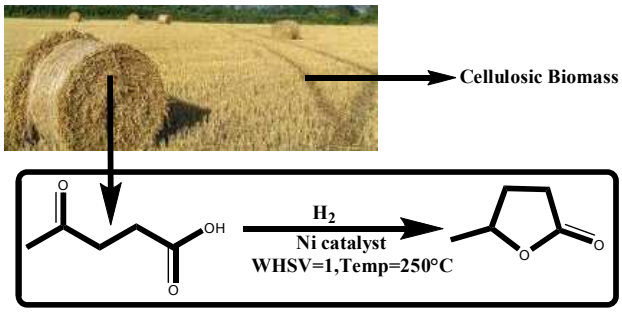

A Ni/SiO_2 catalyst is found to be effective for the hydrogenation of levulinic acid to yield γ- valerolactone with quantitative yield in vapour phase conditions at atmospheric pressure without any additive.